Stabilization of thermogravitational flows by magnetic field and surface tension

D. Henry[a)]
Laboratoire de Mécanique des Fluides et d'Acoustique, UMR-CNRS 5509, Ecole Centrale de Lyon / Université Claude Bernard—Lyon 1, ECL-Boite Postale 163, 69131 Ecully Cedex, France

S. Kaddeche
Institut National des Sciences Appliquées et de Technologie, BP 676, 1080 Tunis Cedex, Tunisia

H. BenHadid
Laboratoire de Mécanique des Fluides et d'Acoustique, UMR-CNRS 5509, Ecole Centrale de Lyon / Université Claude Bernard—Lyon 1, ECL-Boite Postale 163, 69131 Ecully Cedex, France

(Received 28 October 2004; accepted 14 March 2005; published online 27 April 2005)

The influence of a vertical magnetic field and of surface tension on the stability of thermogravitational convection in an infinite layer subject to a horizontal temperature gradient is investigated through a linear stability analysis. Magnetic field is found to strongly stabilize the flow, as well as surface tension if thermocapillary effects contribute to increase the velocity at the upper surface of the layer. This strong stabilization is mainly connected to the modifications of the basic flow profile. A simple model based on the existence of an inflexion point in the velocity profile is proposed which qualitatively depicts these results. © *2005 American Institute of Physics*.
[DOI: 10.1063/1.1901724]

I. INTRODUCTION

Natural convection of metallic liquids subject to a horizontal temperature gradient is often involved in various engineering applications such as material processing technologies and also in the geophysical domain. The stability of these fluid motions, commonly called the Hadley circulation, is a crucial problem since the transitions are responsible of great changes in the flow characteristics.[1] If we consider the particular case of crystal growth applications, it is well known that the melt flow can significantly affect the homogeneity of the grown crystal by inducing undesirable striations due to the transition from laminar to time dependent convection.[2,3] The possibility to delay such a transition and to have a certain control on the flow seems to be a promising opportunity to achieve a significant progress, especially in material processing technologies.

It is now well known that the use of a magnetic field generally allows both the braking of the flow and the damping of the instabilities when the fluid involved is electrically conducting as in the case of the liquid metals used for crystal growth applications. The action of a magnetic field on such convective flows has been the subject of many studies. Experimental investigations have been performed by Hurle *et al.*,[4] Juel *et al.*,[5] Davoust *et al.*,[6] and Tagawa and Ozoe.[7] They concern gallium or mercury heated flows in completely confined parallelepipedic or cylindrical cavities, except in the case of Hurle *et al.*[4] where the upper surface of the fluid is only partially covered. A more recent work by Hof *et al.*[8] concerns the action of the magnetic field on the oscillatory instabilities appearing in such confined parallelepipedic cavities. A strong damping effect is observed corresponding to exponential variations of the thresholds with the increase of the magnetic field intensity. Among the numerical studies, we can cite the works of BenHadid *et al.*[9,10] who have investigated the effect of a vertical magnetic field on the laminar convection occurring in parallelepipedic cavities subject to a horizontal temperature gradient by considering one-, two-, and three-dimensional models. In the case of horizontally extended cavities, BenHadid *et al.*[9] as well as Kaddeche *et al.*[11] have established characteristic laws for the critical threshold parameters as a function of the magnetic field strength, respectively, for open cavities without surface tension and for confined cavities. Priede and Gerbeth[12,13] have achieved a similar work but in the case of a pure thermocapillary convection.

To our knowledge, the effect of a magnetic field on the stability of Hadley natural convection due to the combined action of buoyancy and capillary forces has never been treated. The only investigations in this field consider the laminar damping of this type of flow by a vertical magnetic field.[9,10] Nevertheless, when no magnetic field is applied, the thermocapillary-buoyancy convection was analyzed numerically by Mundrane and Zebib[14,15] and experimentally by Gillon and Homsy.[16] Mundrane and Zebib[14] have proved that varying the thermocapillary effect leads under certain conditions to a transition from two-dimensional to three-dimensional flows. This important result was confirmed by the experimental study of Gillon and Homsy.[16] By means of a two-dimensional model, Mundrane and Zebib[15] have then pointed out a stabilization of the flow when thermocapillarity

[a)]Author to whom correspondence should be addressed. Electronic mail: daniel.henry@ec-lyon.fr

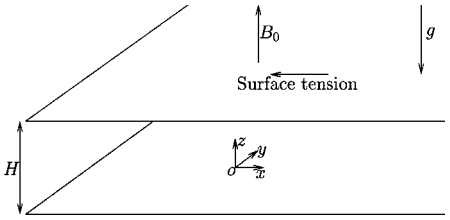

FIG. 1. Studied configuration.

acts in conjunction with buoyancy, a destabilizing effect when thermocapillarity is slightly opposite to buoyancy and again a stabilization when this opposite effect is stronger. At last we can mention the detailed experimental work recently performed by Camel *et al.*[17] on Marangoni flows in molten and solidifying Sn and Sn–Bi layers heated from the side. In their situation, the buoyancy convection remains negligible compared to the thermocapillary convection because of the small thickness of the layer. When directional solidification of alloys is performed, important modifications of the flow (as flow reversal) are observed due to concentration effects generated by the solute rejected ahead of the growth front.

In this paper, we will consider the combined thermogravitational and thermocapillary convection under magnetic field. More precisely, we want to investigate the double effect of a vertical magnetic field and of surface tension on the stability of thermogravitational convection in an infinite layer subject to a horizontal temperature gradient. The objective is to see how controlled modifications of the velocity profiles (induced either by magnetic field or by surface tension) can strongly change the stability of the flow. The paper is organized as follows. The formulation of the problem will be presented in Sec. II, followed by the numerical approach for linear stability analysis in Sec. III. The linear stability results are then detailed in Sec. IV. Section V is then devoted to an energy analysis of the perturbations at their critical thresholds, allowing to get a deeper physical understanding of the instability mechanisms. At last, a discussion of the results in connection with a simple approach based on the inviscid theory is proposed in Sec. VI.

II. GOVERNING EQUATIONS AND BASIC FLOW

We consider a viscous electrically conducting fluid with a constant electric conductivity σ_e contained in a shallow cavity (Fig. 1) subject to a horizontal temperature gradient $\boldsymbol{\nabla}\tilde{T}$ along x and an external vertical constant magnetic field $\boldsymbol{B_0}$. The fluid is assumed to be Newtonian with constant kinematic viscosity ν and thermal diffusivity κ. According to Boussinesq approximation, the fluid density is considered as constant except in the buoyancy term where it is taken as temperature dependent according to the law $\rho=\rho_0[1-\beta(\tilde{T}-\tilde{T}_0)]$ where β is the thermal expansion coefficient and $\tilde{T}_0$ a reference temperature. The fluid layer of height H is bounded at the bottom by a rigid surface while the top surface, open to ambient air, is subject to thermocapillary effect. The surface tension σ at this liquid-air interface considered as a plane, nondeformable boundary is assumed to be a linear function of the temperature, $\sigma=\sigma_0[1-\gamma(\tilde{T}-\tilde{T}_0)]$, where $\gamma=-(1/\sigma_0)\times(\partial\sigma/\partial\tilde{T})$ is generally a positive constant. The assumption of flat top surface for liquid metal flows has been discussed by BenHadid and Roux.[18] They indicate that the free-surface deformation is generally very small due to a high surface tension coefficient.

In what follows, Gr is the Grashof number ($\mathrm{Gr}=g\beta\boldsymbol{\nabla}\tilde{T}H^4/\nu^2$), Re is the Reynolds–Marangoni number [$\mathrm{Re}=(-\partial\sigma/\partial\tilde{T})\boldsymbol{\nabla}\tilde{T}H^2/\rho_0\nu^2$], Pr is the Prandtl number ($\mathrm{Pr}=\nu/\kappa$), and Ha is the Hartmann number ($\mathrm{Ha}=|\boldsymbol{B_0}|H\sqrt{\sigma_e/\rho_0\nu}$).

Since in most laboratory experiments the magnetic Reynolds number ($\mathrm{Re}_m=\mu\sigma_e\tilde{V}_0H$ where μ is the magnetic permeability and $\tilde{V}_0$ a characteristic velocity) is very small, the induced magnetic field b is negligible, and the magnetic field $\boldsymbol{B}$ can then be taken as constant and equal to the applied magnetic field $\boldsymbol{B_0}$.[11]

We consider $H, H^2/\nu, \nu/H, \rho_0\nu^2/H^2, \boldsymbol{\nabla}\tilde{T}H, \nu|\boldsymbol{B_0}|$ and $\sigma_e\nu|\boldsymbol{B_0}|/H$, as scales for length, time, velocity, pressure, temperature, induced electric potential, and induced current, respectively. The dimensionless equations are then

$$\boldsymbol{\nabla}\cdot\boldsymbol{V}=0, \tag{1}$$

$$\frac{\partial\boldsymbol{V}}{\partial t}+(\boldsymbol{V}\cdot\boldsymbol{\nabla})\boldsymbol{V}=-\boldsymbol{\nabla}P+\boldsymbol{\nabla}^2\boldsymbol{V}+\mathrm{Gr}Te_z+\mathrm{Ha}^2\boldsymbol{J}\times\boldsymbol{e_z}, \tag{2}$$

$$\frac{\partial T}{\partial t}+(\boldsymbol{V}\cdot\boldsymbol{\nabla}T)=\frac{1}{\mathrm{Pr}}\boldsymbol{\nabla}^2T, \tag{3}$$

where the dimensionless variables are the velocity vector [$\boldsymbol{V}=(U,V,W)$], the pressure P, and the temperature T, and $\boldsymbol{e_z}$ is the unit vector in the z vertical direction. In the equation of motion (2), the body force $\mathrm{Ha}^2\boldsymbol{J}\times\boldsymbol{e_z}$ is the Lorentz force due to the interaction between the induced electric current density $\boldsymbol{J}$ and the applied magnetic field $\boldsymbol{B_0}$. The dimensionless electric current density $\boldsymbol{J}$ is given by Ohm's law for a moving fluid:

$$\boldsymbol{J}=\boldsymbol{E}+\boldsymbol{V}\times\boldsymbol{e_z}, \tag{4}$$

where $\boldsymbol{E}=-\boldsymbol{\nabla}\Phi$ is the dimensionless electric field and Φ the dimensionless electric potential. Combining the continuity equation for electric current density, $\boldsymbol{\nabla}\cdot\boldsymbol{J}=0$, and Ohm's law (4) leads to the equation governing the electric potential, which can be written in dimensionless form as

$$\boldsymbol{\nabla}^2\Phi=\boldsymbol{\nabla}\cdot(\boldsymbol{V}\times\boldsymbol{e_z}). \tag{5}$$

The mechanical boundary conditions are no-slip conditions at the rigid bottom boundary (located at $z=-0.5$), $\boldsymbol{V}=0$, and conditions on the shear stress for equilibrium at the upper surface ($z=0.5$), $\partial U/\partial z=-\mathrm{Re}\,\partial T/\partial x$, and $\partial V/\partial z=-\mathrm{Re}\,\partial T/\partial y$. The surface tension is assumed to be high enough so that the free surface may be considered as plane, nondeformable and able to support normal stress differences (see BenHadid and Roux[18] for further discussion of this point). For both the thermal and the electric boundary conditions, limit cases are

generally considered, either perfectly conducting or perfectly insulating.

Generally, in a real situation, two opposite vertical boundaries are maintained at different temperatures, T_1 and $T_2 \geqslant T_1$, creating the horizontal temperature gradient along x. This gradient drives the fluid upward near the hot wall and downward near the cold wall, generating a global circulation inside the cavity. In our study dealing with an infinite layer, the cavity is considered to be infinitely long in both horizontal x and y directions. With this assumption, as discussed in previous works by Hart,[19] Cormack *et al.*,[20] and with applied magnetic field by Garandet *et al.*,[21] BenHadid *et al.*[9] and Kaddeche *et al.*,[11] a permanent parallel flow solution can be found.

For a vertical magnetic field, this parallel flow solution, independent of the electric field as the conservation of the current directly derives from the conservation of the flow, is governed by the following equations:

$$\frac{\partial^3 U_0}{\partial z^3} - \mathrm{Ha}^2 \frac{\partial U_0}{\partial z} - \mathrm{Gr} = 0, \tag{6}$$

$$\frac{\partial^2 T_0}{\partial z^2} = \mathrm{Pr} U_0. \tag{7}$$

The analytical expressions obtained for open cavities when taking into consideration surface tension effect are

$$U_0(z) = \mathrm{Gr}\left(C_1 \sinh(\mathrm{Ha}z) + C_2 \cosh(\mathrm{Ha}z) - \frac{1}{\mathrm{Ha}^2} z + C_3 \right), \tag{8}$$

$$T_0(x,z) = x + \mathrm{GrPr}\left(\frac{C_1}{\mathrm{Ha}^2} \sinh(\mathrm{Ha}z) + \frac{C_2}{\mathrm{Ha}^2} \cosh(\mathrm{Ha}z) - \frac{1}{\mathrm{Ha}^2} \frac{z^3}{6} + C_3 \frac{z^2}{2} + C_4 z + C_5 \right), \tag{9}$$

with

$$C_1 = \frac{1}{D}\left[\left(\frac{\mathrm{Re}}{\mathrm{Gr}} - \frac{1}{\mathrm{Ha}^2} \right) \cosh(\mathrm{Ha}/2) + \left(\frac{2}{\mathrm{Ha}^3} - \frac{1}{2\mathrm{Ha}} - \frac{2\,\mathrm{Re}}{\mathrm{GrHa}} \right) \sinh(\mathrm{Ha}/2) \right],$$

$$C_2 = \frac{1}{D}\left[\frac{1}{2\mathrm{Ha}} \cosh(\mathrm{Ha}/2) + \left(\frac{\mathrm{Re}}{\mathrm{Gr}} - \frac{1}{\mathrm{Ha}^2} \right) \times \sinh(\mathrm{Ha}/2) \right], \quad C_3 = \frac{-2\sinh(\mathrm{Ha}/2)}{\mathrm{Ha}} C_2,$$

$$C_4 = \frac{1}{24\mathrm{Ha}^2} - \frac{2\sinh(\mathrm{Ha}/2)}{\mathrm{Ha}^2} C_1, \quad \text{conducting case},$$

$$C_4 = \frac{1}{8\mathrm{Ha}^2} - \frac{\cosh(\mathrm{Ha}/2)}{\mathrm{Ha}} C_1, \quad \text{insulating case},$$

and $D = \sinh(\mathrm{Ha}) - \mathrm{Ha}\cosh(\mathrm{Ha})$. C_5 is a constant not necessary in our investigations because only temperature derivatives are used.

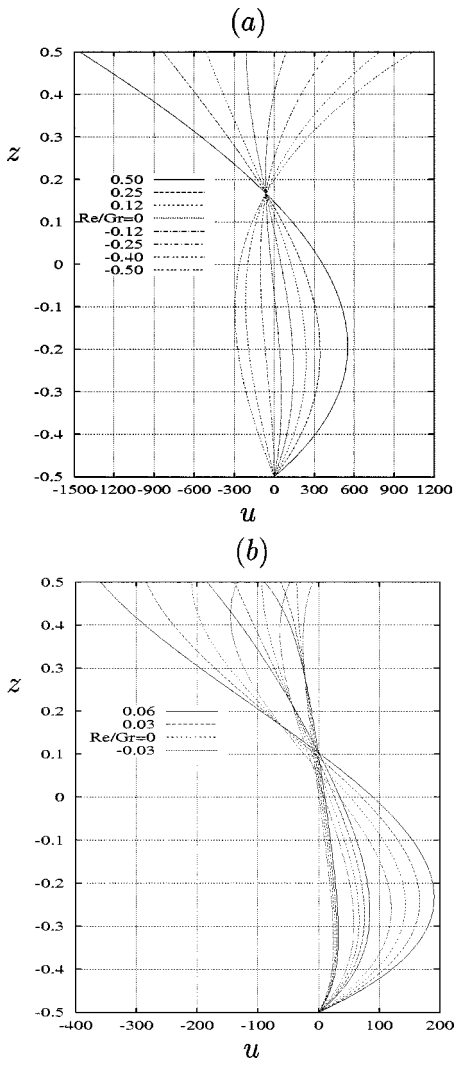

FIG. 2. Velocity profiles for the thermogravitational convection in a layer under the influence of a vertical magnetic field and thermocapillary effects. (a) Velocity profiles for Ha=0 on a large range of Re/Gr ratios to show the strong but regular modifications of the profiles when Re/Gr is changed; (b) velocity profiles for different Ha (Ha=0, 5, and 10) and different Re/Gr ratios to point out the influence of Ha on the modifications of the profiles. All these profiles are obtained for Gr=10 000.

The corresponding velocity profiles are given in Fig. 2 in the conducting case for Gr=10000, Pr=0.02, and for different values of Ha and Re/Gr, Fig. 2(a) showing the variation of these profiles with Re/Gr for Ha=0 and Fig. 2(b) pointing out the influence of Ha on these variations.

III. NUMERICAL APPROACH

The stability of the basic flow solution (8) and (9) is investigated here in a general way by a linear analysis. The solution of the three dimensional problem is written as

$$(\boldsymbol{V}, P, T, \Phi) = (\boldsymbol{V_0}, P_0, T_0, \Phi_0) + (\mathbf{v}, p, \theta, \phi), \tag{10}$$

i.e., the sum of the basic flow quantities and perturbations. Substitution into Eqs. (1)–(5) and linearization with respect to the perturbations yield

$$\boldsymbol{\nabla} \cdot \mathbf{v} = 0, \tag{11}$$

$$\frac{\partial \mathbf{v}}{\partial t} + (\boldsymbol{V_0} \cdot \boldsymbol{\nabla})\mathbf{v} + (\mathbf{v} \cdot \boldsymbol{\nabla})\boldsymbol{V_0} = -\boldsymbol{\nabla} p + \boldsymbol{\nabla}^2 \mathbf{v} + \mathrm{Gr}\theta \boldsymbol{e_z} + \mathrm{Ha}^2(-\boldsymbol{\nabla}\phi + \mathbf{v} \times \boldsymbol{e_z}) \times \boldsymbol{e_z}, \tag{12}$$

$$\frac{\partial \theta}{\partial t} + \boldsymbol{V_0} \cdot \boldsymbol{\nabla}\theta + \mathbf{v} \cdot \boldsymbol{\nabla} T_0 = \frac{1}{\mathrm{Pr}} \boldsymbol{\nabla}^2 \theta, \tag{13}$$

$$\boldsymbol{\nabla}^2 \phi = \boldsymbol{e_z} \cdot (\boldsymbol{\nabla} \times \mathbf{v}), \tag{14}$$

where $\boldsymbol{V_0} = (U_0, 0, 0)$.

Only boundary conditions in the z direction (for $z = -0.5$ and $z = 0.5$) are needed because we use periodic disturbances in the horizontal x and y directions. These conditions are no-slip boundary conditions at $z = -0.5$, $\mathbf{v} = 0$; shear stress equilibrium condition at $z = 0.5$, $\partial u/\partial z = -\mathrm{Re}\,\partial\theta/\partial x$, $\partial v/\partial z = -\mathrm{Re}\,\partial\theta/\partial y$; conducting or insulating thermal boundary conditions: $\theta = 0$ or $\partial\theta/\partial z = 0$, respectively; conducting or insulating electric boundary conditions: $\phi = 0$ or $\boldsymbol{j} \cdot \boldsymbol{e_z} = 0$, respectively.

The linear stability study performed here consists, for fixed values of the Hartmann number Ha, the Prandtl number Pr and the Reynolds–Marangoni number Re, of the determination of Gr_c, the critical value of Gr beyond which the basic flow loses its stability. In our situation, the perturbations can be developed in normal modes given by

$$(\mathbf{v}, p, \theta, \phi) = (\mathbf{v}, p, \theta, \phi)(z) e^{i(hx+ky)+\omega t}, \tag{15}$$

where h and k are real wavenumbers in the longitudinal x and transverse y directions, respectively, and $\omega = \omega_r + i\omega_i$ is a complex eigenvalue. The real part of ω represents an amplification rate and its imaginary part an oscillation frequency. Using these disturbances, the set of Eqs. (11)–(14) is transformed into a generalized eigenvalue problem which depends on h, k, Pr, Gr, Re, and Ha. It is solved with the spectral Tau–Chebyshev method by means of a numerical procedure using the QZ eigenvalue solver of the NAG library. From the thresholds Gr_0 (Pr, Ha, Re, h, k) (values of Gr for which an eigenvalue has a real part equal to zero whereas all the other eigenvalues have negative real parts), the critical Grashof number Gr_c can be obtained after minimization with respect to h and k ($\mathrm{Gr}_c = \inf_{(h,k)\in\mathcal{R}^2} \mathrm{Gr}_0$ (Pr, Ha, Re, h, k)). Here, we will only consider the two-dimensional transverse instabilities with $k = 0$ which are the first instabilities to arise for very low Prandtl numbers and which are the most sensitive to the action of the magnetic field.[11] Minimization will then only depend on h. Moreover, these instabilities are independent of the potential ϕ and of the electric boundary conditions.[11]

The critical Grashof numbers have been determined by expanding the variables in the z direction in a Chebyshev series with 30 to 40 collocation points. This was sufficient for an accurate determination of the linear stability characteristics.

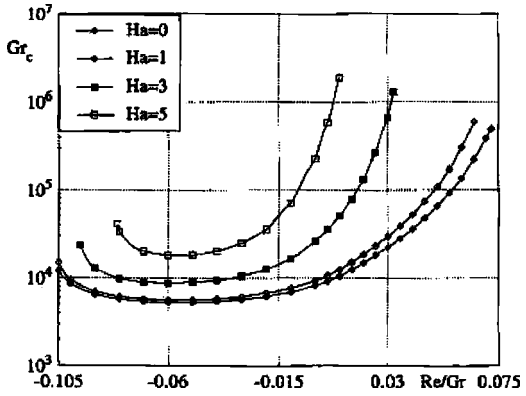

FIG. 3. Variation of the thresholds Gr_c as a function of Re/Gr for different values of Ha (Pr=0.02).

IV. LINEAR STABILITY RESULTS

The effect of a uniform vertical magnetic field on the stability of a laterally heated layer with a stress-free surface at the upper boundary has already been studied in a previous study.[9] The results have shown the strong stabilization effect obtained by the magnetic field, the critical thresholds evolving as Ha^2 for the longitudinal three-dimensional modes and as $\exp(\mathrm{Ha}^2/9)$ for the transverse two-dimensional modes (Pr=0.001). These results look qualitatively similar to those obtained in a cavity with a rigid upper boundary (denoted as the rigid situation), with comparable stabilization laws for both instabilities,[11] but, as was already shown without magnetic field, the transverse two-dimensional instability is stationary in the rigid situation whereas it is oscillatory in the free-surface case.

In this paper, we consider the situation of a laterally heated layer subject to surface tension at the upper boundary, and focus on the two-dimensional modes of dynamical origin. We want to study the combined effect of vertical magnetic field and surface tension on the stability of these modes (thermally conducting case, Pr=0.02). The stability thresholds corresponding to the critical value of the Grashof number Gr_c are given in Fig. 3 as a function of Re/Gr, the ratio of the Reynolds–Marangoni number by the Grashof number, for different Ha values. Note that a positive ratio Re/Gr indicates that surface tension drives the flow in the same di-

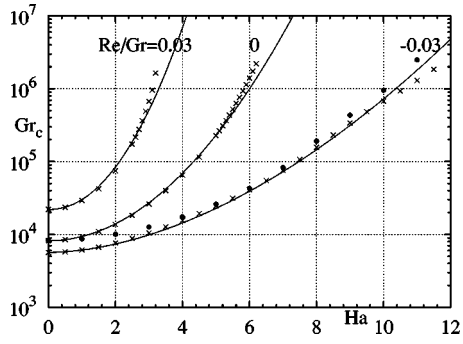

FIG. 4. Variation of the thresholds Gr_c as a function of Ha for three values of Re/Gr (Pr=0.02). The symbols (X) correspond to the calculated results and the lines to well-correlated characteristic laws given in the text. For comparison, the symbols (•) indicate the results for the rigid situation.

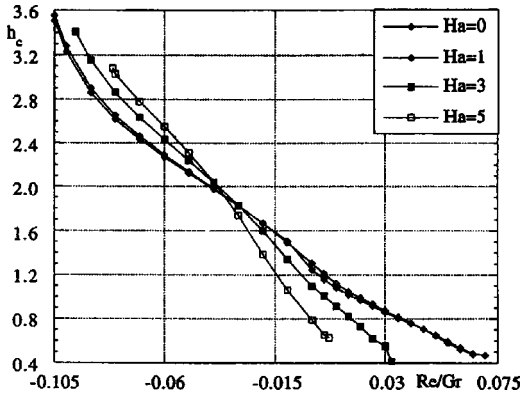

FIG. 5. Variation of the critical wavenumbers h_c as a function of Re/Gr for different values of Ha (Pr=0.02).

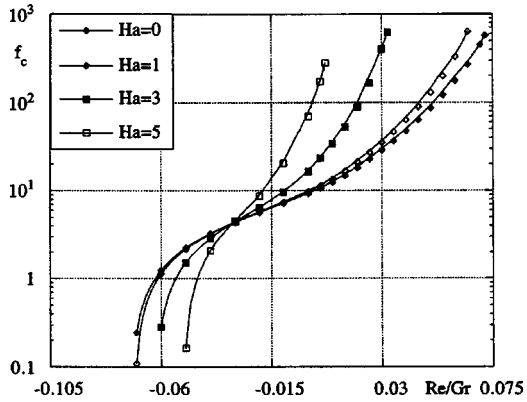

FIG. 7. Variation of the critical frequency f_c as a function of Re/Gr for different values of Ha (Pr=0.02).

rection as buoyancy. In this situation we will speak of driving Marangoni forces, whereas for $\mathrm{Re/Gr} \leqslant 0$ we will speak of opposing Marangoni forces. Figure 3 first shows that the neutral stability curves are shifted upward, corresponding to stabilization, when the Hartmann number is increased. Concerning the influence of the thermocapillary forces, when they act in support of buoyancy forces ($\mathrm{Re/Gr} > 0$), stabilization is observed corresponding to a strong increase of the thresholds, this increase being still more pronounced when Ha is stronger. When thermocapillary forces act in opposition to buoyancy forces ($\mathrm{Re/Gr} < 0$), the influence depends on the relative importance of these two driving forces. A destabilizing effect is first observed for relatively small thermocapillary contribution, until Gr_c reaches a minimum for $\mathrm{Re/Gr} \sim 0.06$. Beyond this value, the critical Grashof number increases again indicating a stabilizing effect. Note that the minimum of Gr_c is reached for about the same value of Re/Gr, independently of the value of the Hartmann number. This type of dependence of the thresholds with Re/Gr is similar to what has been obtained by Mundrane and Zebib[15] for a two-dimensional cavity.

The stabilizing effect of the magnetic field is emphasized in Fig. 4 where the instability thresholds are given as a function of Ha for different values of Re/Gr, each instability being mentioned up to the limit value of Ha for which it can be observed (the disappearance of the instability is similar to what has been observed for these two-dimensional modes in the rigid situation[11]). For all cases, we note a strong stabilization by the magnetic field, this stabilization being still more efficient when Re/Gr is increased, assuming that $\mathrm{Re/Gr} \geqslant -0.06$. The domain of Ha where the instability can be observed is also reduced when Re/Gr is increased. In Fig. 4, the evolution of the thresholds in the stress-free situation (Re/Gr=0) is also compared to the evolution in the rigid situation: despite a slightly smaller threshold for Ha=0 ($\mathrm{Gr}_c = 8213$ compared to 8271), the stress-free situation is much more strongly stabilized by the magnetic field. The stabilization is still stronger for positive values of Re/Gr with, for example, for Re/Gr=0.03, an increase of Gr_c by two decades for values of Ha less than 4. All these variations of the thresholds with Ha are close to $\exp(\mathrm{Ha}^2)$ laws. The correlated curves given in Fig. 4 correspond to $\mathrm{Gr}_c = \mathrm{Gr}_{c0}\exp(\mathrm{Ha}^{1.8}/13)$ for Re/Gr=−0.03, $\mathrm{Gr}_c = \mathrm{Gr}_{c0}\exp(\mathrm{Ha}^2/7.5)$ for Re/Gr=0, and $\mathrm{Gr}_c = \mathrm{Gr}_{c0}\exp(\mathrm{Ha}^{2.1}/3.2)$ for Re/Gr=0.03 (Gr_{c0} is each time the corresponding value of Gr_c at Ha=0). An important point of the results is then that the conjunction of driving Marangoni forces with vertical magnetic field is particularly efficient in stabilizing the two-dimensional instabilities. At last, in Fig. 4 we can see that the evolution of the thresholds in the rigid situation is closer to the evolution in the case Re/Gr =−0.03. This can be connected to the fact that, as can be seen in Fig. 2, for small negative values of Re/Gr($\mathrm{Re/Gr} \geqslant -0.08$) the velocity at the upper boundary decreases and gets closer to the zero velocity condition imposed in the rigid situation.

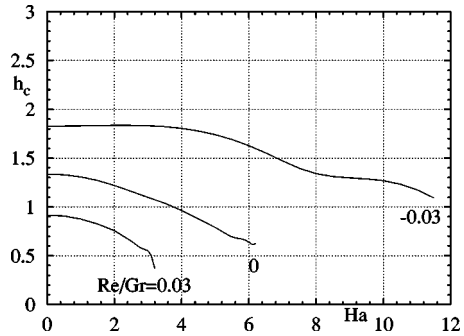

FIG. 6. Variation of the critical wavenumbers h_c as a function of Ha for three values of Re/Gr (Pr=0.02).

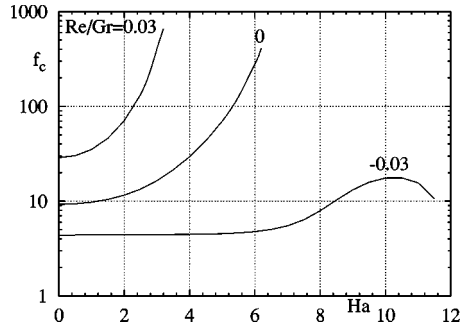

FIG. 8. Variation of the critical frequency f_c as a function of *Ha* for three values of Re/Gr (Pr=0.02).

TABLE I. Energy analysis in the stress-free case (Re/Gr=0) for the two-dimensional modes with vertical magnetic field at Pr=0.02.

Ha	K'_f	K'_b	K'_m	Θ'_{f1}	Θ'_{f2}	R_d
0	1.0400	−0.0400	0.0000	0.0840	0.9160	10.871
2	1.1519	−0.0613	−0.0905	0.1154	0.8846	6.969
3	1.2771	−0.1019	−0.1752	0.1806	0.8194	4.094
4	1.4260	−0.1903	−0.2357	0.3391	0.6609	1.951
5	1.5712	−0.3382	−0.2330	0.6129	0.3871	0.606
5.5	1.6873	−0.4852	−0.2021	0.7694	0.2306	0.226
6	1.9425	−0.7867	−0.1558	0.8912	0.1088	0.061

Concerning the critical wavenumber h_c (Fig. 5), it quite regularly decreases with the increase of Re/Gr, corresponding to longer wavelengths for the perturbations. The influence of Ha which corresponds to an increase of the wavelengths in the domain of Re/Gr around 0 (as in the rigid situation) is found to change for $\mathrm{Re/Gr} \leqslant -0.035$. Some precisions on the variation of the wavenumber with Ha are given in Fig. 6. In any case, because of the small range of Ha where the instability exists, the decrease shown remains limited, corresponding at the most to an increase of the wavelengths by a factor of 2. Vertical magnetic field and driving Marangoni forces then favor the existence of longer cells in the cavity.

Finally, the variation of the critical frequency f_c of the instability is given in Figs. 7 and 8, first as a function of Re/Gr, then as a function of Ha. The frequency is strongly increased for increasing driving Marangoni forces ($\mathrm{Re/Gr} \geqslant 0$) and increasing Ha. This behavior is changed for smaller Re/Gr with, in particular, a rather small variation of the frequency with Ha for Re/Gr=−0.03 and a strong decrease of the frequency for Re/Gr around −0.06. This decrease can still be connected to the fact that the velocity at the upper boundary gets closer to the zero velocity condition imposed in the rigid situation, a situation where the frequency is zero (steady transition).

The major conclusion we can draw is that both magnetic field and driving Marangoni forces strongly stabilize the flow, leading to critical oscillatory modes characterized by longer cells and stronger frequencies.

V. ENERGY ANALYSES

Energy analyses have been used to characterize the increase of the thresholds when Re/Gr and Ha are increased. We have chosen three values of Re/Gr, Re/Gr=−0.03, 0, and 0.03, and different values of Ha between 0 and 10. The results are presented first as energy balances and then as energetic contributions to the critical Grashof number.

A. Energy balances

By multiplying the linear stability equations (12) and (13) by $\mathbf{v}^*$ (the complex conjugate of the velocity perturbation) and θ^* (the complex conjugate of the temperature perturbation), respectively, and after integration along z and some simplifications, energy equations concerning the fluctuating kinetic energy and thermal energy can be derived. From these equations, for any instabilities at their critical thresholds, normalized energy balances can be obtained[11] which we can write as

$$K'_f + K'_b + K'_m = 1, \tag{16}$$

$$\Theta'_{f1} + \Theta'_{f2} = 1, \tag{17}$$

where $K'_f = -\mathcal{R}(\int_z w\ \partial U_0/\partial z\ u^* dz)/|K_d|$ is the production of fluctuating kinetic energy by shear of mean flow, $K'_b = \mathcal{R}(\mathrm{Gr}\int_z \theta w^* dz)/|K_d|$ the production of fluctuating kinetic energy by buoyancy forces and $K'_m = \mathcal{R}(\mathrm{Ha}^2 \int_z [(-\boldsymbol{\nabla}\phi + \mathbf{v} \times \boldsymbol{e}_{\boldsymbol{B}_0}) \times \boldsymbol{e}_{\boldsymbol{B}_0}] \mathbf{v}^* dz)/|K_d|$ the dissipation of fluctuating kinetic energy by magnetic forces, all these terms being normalized

TABLE II. Energy analysis in the case with opposing Marangoni forces (Re/Gr=−0.03) for the two-dimensional modes with vertical magnetic field at Pr=0.02.

Ha	K'_f	K'_b	K'_m	Θ'_{f1}	Θ'_{f2}	R_d
0	1.0334	−0.0334	0.0000	0.0619	0.9381	16.540
2	1.1403	−0.0453	−0.0950	0.0729	0.9271	12.715
3	1.2681	−0.0630	−0.2051	0.0877	0.9123	9.519
4	1.4395	−0.0938	−0.3458	0.1104	0.8896	6.647
5	1.6514	−0.1458	−0.5055	0.1446	0.8554	4.388
6	1.8998	−0.2339	−0.6659	0.1974	0.8026	2.734
8	2.4690	−0.6487	−0.8203	0.4444	0.5556	0.837
10	2.9218	−1.2017	−0.7201	0.7678	0.2322	0.211
11	2.9648	−1.2590	−0.7058	0.8054	0.1946	0.107

TABLE III. Energy analysis in the case with driving Marangoni forces (Re/Gr=0.03) for the two-dimensional modes with vertical magnetic field at Pr=0.02.

Ha	K'_f	K'_b	K'_m	Θ'_{f1}	Θ'_{f2}	R_d
0	1.0668	−0.0668	0.0000	0.2024	0.7976	4.840
1	1.0971	−0.0791	−0.0180	0.2452	0.7548	3.841
2	1.1722	−0.1186	−0.0536	0.4106	0.5894	1.681
2.5	1.2205	−0.1575	−0.0630	0.5583	0.4417	0.681
3	1.3754	−0.3217	−0.0537	0.7839	0.2161	0.123
3.2	1.4609	−0.4124	−0.0486	0.8466	0.1534	0.046

by the viscous dissipation of fluctuating kinetic energy $K_d = \mathcal{R}(\int_z \boldsymbol{\nabla}^2 \mathbf{v}\mathbf{v}^* dz)$, and where $\Theta'_{f1} = -\mathcal{R}(\int_z w\ \partial T_0/\partial z\ \theta^* dz)/|\Theta_d|$ is the production of fluctuating thermal energy by vertical transport of temperature, and $\Theta'_{f2} = -\mathrm{Re}(\int_z u\ \partial T_0/\partial x\ \theta^* dz)/|\Theta_d|$ the production of fluctuating thermal energy by horizontal transport of temperature, these two last terms being normalized by the dissipation of fluctuating thermal energy by conduction $\Theta_d = \mathcal{R}((1/\mathrm{Pr})\int_z \boldsymbol{\nabla}^2 \theta\theta^* dz)$ ($\mathcal{R}$ is used to denote the real part). As in Kaddeche *et al.*,[11] in order to compare the kinetic energy contributions to the thermal energy contributions, a ratio of the respective dissipation terms is given as $R_d = K_d/(\mathrm{Gr}_c \Theta_d)$.

The energy balances for Re/Gr=0 are given in Table I as a function of Ha. In the kinetic energy balance (which is dominant without magnetic field), the increase of Ha induces a relatively moderate increase of the stabilizing magnetic term K'_m, but a stronger increase of the stabilizing buoyancy term K'_b. To compensate these increases, the destabilizing shear term K'_f increases too. In the thermal energy balance, the main effect is the strong increase of Θ'_{f1}, the destabilizing vertical transport of temperature, this term even becoming the dominant destabilizing term for large enough Ha. This last effect seems associated with values of R_d becoming smaller than 1. These evolutions with Ha are quite similar to those obtained in the rigid situation, but they occur more quickly.

For Re/Gr=−0.03 (Table II), the evolution with Ha of the buoyancy term is weaker and that of the Lorentz forces term a little stronger, whereas the thermal variations with Ha are weaker. It is the contrary for Re/Gr=0.03 (Table III), with stronger buoyancy term evolution, weaker Lorentz forces term evolution and stronger thermal variations. In fact, the global evolutions obtained up to the limit Ha value are stronger for Re/Gr=−0.03, because the instability, less stabilized, occurs on a wider range of Ha in this case. In any of these cases, the Lorentz forces contribution levels off as Ha is increased, so that it becomes dominated by the stabilizing buoyancy contribution.

B. Energetic contributions to the critical Grashof number

The previous analysis has shown how the energy balances between the different production and dissipation terms evolve when a vertical magnetic field or surface tension is applied. It would also be interesting to understand what are the main reasons for the very strong stabilizing effect obtained. For that, following what has been done by Kaddeche *et al.*[11] and noting that K'_f (through U_0) and K'_b are proportional to Gr ($K'_f = \mathrm{Gr}\ k'_f$ and $K'_b = \mathrm{Gr}\ k'_b$), we can use Eq. (16) applied for Ha non zero and Ha=0 (subscript 0) to derive an expression for $\mathrm{Gr}/\mathrm{Gr}_0$:

$$\frac{\mathrm{Gr}}{\mathrm{Gr}_0} = R_1 R_2, \tag{18}$$

where

$$R_1 = \left(\frac{k'_{f_0} + k'_{b_0}}{k'_f + k'_b} \right), \quad R_2 = 1 - K'_m. \tag{19}$$

As $K'_m < 0$, the action of the magnetic field will increase Gr by the increase of R_2 in connection with the Lorentz forces. This action of the magnetic field will also modify the velocity profile, leading to a decrease of k'_f (to which $|k'_b|$, less strong, is subtracted) and thus to an increase of R_1 and of Gr. Surface tension will also modify the velocity profile and modify Gr through R_1.

The results are presented in Tables IV–VI where for each case are given the evolutions with Ha of R_1, R_2, and $\mathrm{Gr}/\mathrm{Gr}_0 = R_1 R_2$. In the three cases presented, the stabilization by the vertical magnetic field is mainly the consequence of the strong increase of R_1 (in connection with the modifications of the basic velocity profile) and only slightly connected to the stabilizing effect of the Lorentz force. In the case without surface tension (Re/Gr=0, Table IV) the stabilization by magnetic field is much stronger than in the rigid situation (Fig. 4), essentially due to stronger values of R_1.[11] The influence of Re/Gr on the thresholds (increase for

TABLE IV. Characterization of the stabilization by a vertical magnetic field for the two-dimensional modes in the stress-free case (Re/Gr=0) at Pr=0.02.

Ha	R_1	R_2	$\mathrm{Gr}/\mathrm{Gr}_0$
2	1.53	1.09	1.67
3	2.71	1.18	3.18
4	6.41	1.24	7.92
5	22.43	1.23	27.65
5.5	52.82	1.20	63.50
6	147.41	1.16	170.38

TABLE V. Characterization of the stabilization by a vertical magnetic field for the two-dimensional modes in the case with opposing Marangoni forces (Re/Gr=−0.03) at Pr=0.02.

Ha	R_1	R_2	Gr/Gr_0
2	1.23	1.10	1.34
3	1.54	1.21	1.85
5	2.87	1.51	4.33
6	4.36	1.67	7.26
7	7.46	1.79	13.37
9	33.91	1.76	59.83
10	69.41	1.72	119.39
11	134.12	1.71	228.78

Re/Gr=0.03, decrease for Re/Gr=−0.03) is clearly seen to be also connected to the modifications of R_1, the contribution R_2 remaining small in any cases (Tables V and VI).

VI. DISCUSSION

We have seen in the preceding section that the strong modifications of the stability thresholds with Ha and Re/Gr appear to be connected to the modifications of the basic velocity profiles. These profiles have been presented in Fig. 2; Fig. 2(a) shows the variations of these profiles on a large range of Re/Gr values for Ha=0 and Fig. 2(b) shows the variations with Re/Gr for different values of Ha. Figure 2(a) shows the strong influence of Re/Gr on the profiles, variations from 0.5 to −0.5 completely changing the concavity of the profiles, the inflexion point moving from the top of the layer to the bottom. Figure 2(b) shows that small values of Ha are able to strongly accentuate the influence connected to the increase of Re/Gr and corresponding to the displacement of the inflexion point towards the top of the layer. We can also remark that, for a given Ha, the profiles have a fixed point when Re/Gr is varied. The explanation is that, at this point, the Re dependent part of the profiles is zero. The position of this point is dependent on Ha, moving slowly from $z=1/6$ for Ha=0 towards $z=0.5$ for $Ha\to\infty$, with a slow asymptotic variation $z=0.5-\ln(Ha)/Ha$.

The variation of the position of the inflexion point in the velocity profiles is given in Fig. 9(a) as a function of Re/Gr for different values of Ha (Ha=0, 3, 5, and 10). We see that for Ha=0 the variation with Re/Gr is linear, but that this variation changes very quickly with Ha. The most striking feature is that the displacement of the inflexion point towards the top layer at $z=0.5$ is obtained for still smaller positive values of Re/Gr, as Ha is increased.

TABLE VI. Characterization of the stabilization by a vertical magnetic field for the two-dimensional modes in the case with driving Marangoni forces (Re/Gr=0.03) at Pr=0.02.

Ha	R_1	R_2	Gr/Gr_0
2	3.21	1.05	3.39
2.5	7.40	1.06	7.87
2.8	15.56	1.06	16.50
3	28.83	1.05	30.38
3.2	71.07	1.05	74.52

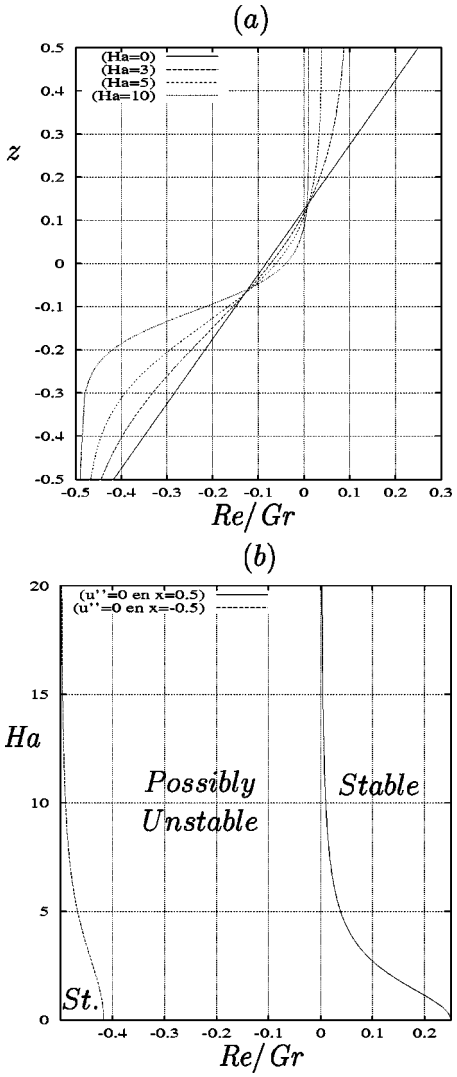

FIG. 9. (a) Variation of the position of the inflexion point in the velocity profiles when Re/Gr is changed for different values of Ha; (b) limits of the profiles with an inflexion point in terms of Re/Gr as a function of Ha, indicating limits of stability in the frame of the inviscid theory.

Simple criteria for the instability of parallel two-dimensional flows have been obtained by Rayleigh, and by Fjortoft (see the work by Drazin and Reid[22]) in the frame of the inviscid theory. Rayleigh's theorem points out that a necessary condition for instability is that the basic velocity profile should have an inflexion point. Fjortoft's theorem, which is more precise, points out that a necessary condition for instability is that the relation $U''(U-U_s)\leqslant 0$ is verified somewhere in the velocity profile, where z_s is a point at which $U''=0$, and $U_s=U(z_s)$.

In the rigid situation, the velocity profiles are symmetric with an inflexion point in the middle of the cavity, and the relation $U''(U-U_s)\leqslant 0$ is verified everywhere in the cavity. The necessary condition for instability is then always verified, and no domain of stability can thus be found from this condition. In the case of an open cavity with surface tension

at the upper fluid boundary, we have seen that the inflexion point moves when the ratio Re/Gr is changed, but we have also verified that in the cases where the inflexion point is present in the velocity profile, the relation $U''(U-U_s) \leqslant 0$ is always verified somewhere in the cavity. Domains of stability will thus only correspond to profiles without any inflexion point. These domains are shown in Fig. 9(b) where the limits of the profiles with an inflexion point are given in terms of Re/Gr as a function of Ha. The most striking result of this analysis in the frame of the inviscid theory is the strong reduction of the instability domain for positive Re/Gr values when Ha is increased. This depicts qualitatively what we obtain in the numerical results, having in mind that the numerical results take into account different effects as viscosity, Lorentz forces, and thermal effects (Pr=0.02), not considered in the frame of the inviscid theory.

VII. CONCLUDING REMARKS

We have investigated the double effect of a vertical magnetic field and of surface tension on the stability of thermogravitational convection in an infinite layer subject to a horizontal temperature gradient. A major observation is that both magnetic field and driving Marangoni forces strongly stabilize the flow with respect to the two-dimensional oscillatory modes of dynamical origin. The evolution of these modes is characterized by longer cells and stronger frequencies. Through an energy analysis, we were able to connect this strong stabilization with the modifications of the basic flow profiles, and not much to the Lorentz force. A detailed analysis of these basic velocity profiles has shown that they have an inflexion point which is quickly displaced towards the upper boundary when magnetic field or driving boundary force is applied. Using Rayleigh's theorem in the frame of the inviscid theory, we have been able to delimit a potentially unstable region and a stable region corresponding to basic velocity profiles without inflexion point. More precisely, we observe a strong reduction of the potentially unstable region for positive Re/Gr values when Ha is increased, which qualitatively depicts the results obtained numerically.

ACKNOWLEDGMENTS

The authors would like to express their grateful thanks to Professor R. Moreau from the MADYLAM of Grenoble, Dr. T. Alboussière from the LGIT of Grenoble, and Dr. J. P. Garandet from C.E.N.G. for fruitful discussions. They also wish to thank Dr. P. Laure from the I.N.L. Nice for helpful suggestions in the numerical calculations.

[1] D. Henry and M. Buffat, "Two- and three-dimensional numerical simulations of the transition to oscillatory convection in low-Prandtl-number fluids," J. Fluid Mech. **374**, 145 (1998).
[2] S. M. Pimputkar and S. Ostrach, "Convective effects in crystals grown from melts," J. Cryst. Growth **55**, 614 (1981).
[3] F. Z. Haddad, J. P. Garandet, D. Henry, and H. BenHadid, "Analysis of unsteady segregation in crystal growth from a melt. Part II: Fluctuating convection velocity," J. Cryst. Growth **220**, 166 (2000).
[4] D. T. J. Hurle, E. Jakeman, and C. P. Johnson, "Convective temperature oscillations in molten gallium," J. Fluid Mech. **64**, 565 (1974).
[5] A. Juel, T. Mullin, H. BenHadid, and D. Henry, "Magnetohydrodynamic convection in molten gallium," J. Fluid Mech. **378**, 97 (1999).
[6] L. Davoust, M. D. Cowley, R. Moreau, and R. Bolcato, "Buoyancy driven convection with a uniform magnetic field. Part 2. Experimental investigation," J. Fluid Mech. **400**, 59 (1999).
[7] T. Tagawa and H. Ozoe, "Enhanced heat transfer rate measured for natural convection in liquid gallium in a cubical enclosure under a static magnetic field," ASME J. Heat Transfer **120**, 1027 (1998).
[8] B. Hof, A. Juel, and T. Mullin (private communication).
[9] H. BenHadid, D. Henry, and S. Kaddeche, "Numerical study of convection in the horizontal Bridgman configuration under the action of a constant magnetic field. Part 1: Two-dimensional flows," J. Fluid Mech. **333**, 23 (1997).
[10] H. BenHadid and D. Henry, "Numerical study of convection in the horizontal Bridgman configuration under the action of a constant magnetic field. Part 2: Three-dimensional flows," J. Fluid Mech. **333**, 57 (1997).
[11] S. Kaddeche, D. Henry, and H. BenHadid, "Magnetic stabilization of the buoyant convection between infinite horizontal walls with a horizontal temperature gradient," J. Fluid Mech. **480**, 185 (2003).
[12] J. Priede and G. Gerbeth, "Hydrothermal wave instability of thermocapillary-driven convection in a coplanar magnetic field," J. Fluid Mech. **347**, 141 (1997).
[13] J. Priede and G. Gerbeth, "Hydrothermal wave instability of thermocapillary-driven convection in a transverse magnetic field," J. Fluid Mech. **404**, 211 (2000).
[14] M. Mundrane and A. Zebib, "Oscillatory buoyant thermocapillary flow," Phys. Fluids **6**, 3294 (1994).
[15] M. Mundrane and A. Zebib, "Two- and three-dimensional buoyant thermocapillary convection," Phys. Fluids A **5**, 810 (1993).
[16] P. Gillon and G. M. Homsy, "Combined thermocapillary-buoyancy convection in a cavity: An experimental study," Phys. Fluids **8**, 2953 (1996).
[17] D. Camel, P. Tison, and J. P. Garandet, "Experimental study of Marangoni flows in molten and solidifying Sn and Sn-Bi layers heated from the side," Eur. Phys. J.: Appl. Phys. **18**, 201 (2002).
[18] H. BenHadid and B. Roux, "Buoyancy- and thermocapillary-driven flows in differentially heated cavities for low-Prandtl-number fluids," J. Fluid Mech. **235**, 1 (1992).
[19] J. E. Hart, "A note on stability of low Prandtl number Hadley circulation," J. Fluid Mech. **132**, 271 (1983).
[20] D. E. Cormack, L. G. Leal, and J. Imberger, "Natural convection in a shallow cavity with differentially heated end walls. Part 1: Asymptotic theory," J. Fluid Mech. **65**, 209 (1974).
[21] J. P. Garandet, T. Alboussière, and R. Moreau, "Buoyancy driven convection in a rectangular enclosure with a transverse magnetic field," Int. J. Heat Mass Transfer **35**, 741 (1992).
[22] P. G. Drazin and W. H. Reid, *Hydrodynamic Stability* (Cambridge University Press, Cambridge, UK, 1981).